Research paper

Stereo-dynamical effects in chemi-ionization reactions of atmospheric O_2 and N_2 molecules promoted by collisions with Ne*($^3P_{2,0}$) atoms

Stefano Falcinelli [a,*], Franco Vecchiocattivi [a], James M. Farrar [b], Brunetto G. Brunetti [c], Simonetta Cavalli [c], Fernando Pirani [c,*]

[a] Department of Civil and Environmental Engineering, University of Perugia, Via G. Duranti 93, 06125 Perugia, Italy
[b] Department of Chemistry, University of Rochester, Rochester, NY 14627, USA
[c] Department of Chemistry, Biology and Biotechnologies, University of Perugia, Via Elce di Sotto 8, 06123 Perugia, Italy

ARTICLE INFO

ABSTRACT

This letter focuses on general aspects of the stereodynamics of chemi-ionization reactions, triggered by collisions of O_2 and N_2 molecules with metastable neon atoms. Basic characteristics of the long-range intermolecular forces involved, some of chemical and others of physical origin, suggest that the weakly bound precursor state, determining the reaction transition state structure and stability, is rather different. Fundamental reaction selectivities are clarified, highlighting differences in the: i) optical potential whose real and imaginary parts must be interdependent; ii) polarizability, quadrupolar moments and orbital representation of the molecules involved, which allow to lay the foundations for future more in-depth investigations.

1. Introduction

The stable closed-shell nature of noble gas atoms Ng accounts for their reluctance towards chemical reactivity [1]. However, when excited in electronic metastable states Ng* atoms assume an open shell structure that, coupled to the high energy content, make them extremely reactive. In particular, they live for a time sufficiently long to give several collisions with other partners leading to a significant reactivity even under rarefied conditions [2–4]. Ng*can be formed by collisions of Ng atoms with cosmic rays and/or energetic electrons and their two body collisions with neutral atomic/molecular M partners can promote chemi-ionization (CHEMI) reactions, from sub-thermal (cold chemistry) [5] up to hyper-thermal (hot chemistry) conditions, with the possible formation of NgM$^+$ (associative ion), Ng + M$^+$ (Penning ion) and electrons. The most highly energetic He* and Ne* atoms trigger CHEMI with most neutral species and in the case of molecular partners also lead to ions coming from the fragmentation of parent M$^+$ [3,4].

Because of their relevance in the balance of microscopic processes occurring in plasmas, electric discharges and laser systems, CHEMI reactions have been investigated in bulk, and under single collision conditions [2–4]. Important experimental findings have been provided by molecular beam experiments where the collision energy dependence of total and partial (i.e. referred to specific reaction channels) ionization

cross sections and of Penning ionization electron spectra (PIES) have been measured. All these findings depend on different features of the optical potential, formerly introduced for the description of nuclear reactive collisions [6], whose real part drives the collision dynamics, while its imaginary part, triggering the passage from neutral reagents to ionic products, accounts for the "opacity" of the system [3,4]. However, despite the relevant work done by eminent research groups [7–14], information on important details of the intermolecular forces controlling the optical potential, especially their dependence on the relative orientation of involved partners, is to date rather limited, providing an incomplete picture of the reaction stereodynamics.

Recently, we have proposed and applied a new/original method for the detailed representation of CHEMI promoted by collisions of Ne* ($^3P_{2,0}$) with Ar, Kr, Xe and such a study provided an internally consistent rationalization of available experimental findings [15–18]. In particular, the proper characterization of the intermolecular forces that drive the atom–atom reaction dynamics cast light on fundamental aspects concerning rearrangement and angular momentum coupling of valence electrons. The results obtained can be considered of general interest for the description of the dynamics of many other elementary chemical reactions. In particular, the application of our method has clearly shown how CHEMI occurs through the competition of two alternative (*direct/indirect*) reaction mechanisms driven by the selectivity of intermolecular

* Corresponding authors.
  E-mail addresses: stefano.falcinelli@unipg.it (S. Falcinelli), fernando.pirani@unipg.it (F. Pirani).

forces involved [17,18]. The *direct mechanism*, dominant at short separation distances of reagents, is basically controlled by chemical forces due to charge (electron) transfer (CT) effects. The *indirect mechanism*, prevalent at large separation distances, originates from weaker forces of more physical origin, such as those due to dispersion, induction-polarization contributions and those promoting spin–orbit and centrifugal-Coriolis effects. Moreover, while the *direct mechanism* controls the evolution of prototype elementary *oxidation reactions* [17,18], the *indirect mechanism* typically triggers *radiative (photo)-ionization processes* [19,20].

This letter reports on one of steps we are following to extend the method to the study of CHEMI reactions of molecules. The present focus is on the correct identification of the nature and strength of intermolecular forces controlling structure and stability of the reaction transition state (TS). It is worth noting that intermolecular forces involved in CHEMI of molecules are usually stronger, more anisotropic and include additional components relative to the atom–atom case [19,21]. Their features are here considered fundamental to correctly identify the real part but also to properly define the nature and role of the imaginary part of the optical potential that triggers the reaction selectivity along each state-to-state channel [16–18].

2. CHEMI of O_2 and N_2

Main focus of this article is on CHEMI of O_2 and N_2 molecules, promoted by collisions with Ne*($^3P_{2,0}$) atoms, that are elementary processes of particular relevance for the balance of phenomena occurring in the atmosphere [22,23] and for which important details on their sterodynamics are still lacking.

As emphasized by Beijerinck and coworkers [24], O_2 and N_2 reagents belong to two rather different classes of CHEMI. In particular, the first group contains molecules as O_2 which show decreasing cross sections with the increase of collision energy, while the second group is formed by those systems, as Ne* –N_2 and Ne* –CO, which exhibit increasing cross sections (see Fig. 1). This experimental finding suggests that the reaction mechanism must be rather different.

Ionization processes of O_2 by metastable He*(2 ^{3}S) and He*(2 ^{1}S) atoms have been experimentally investigated about forty years ago in the thermal collision energy range [25]. It was found that CHEMI of O_2 evolves through parallel reaction channels leading to the formation of O_2^+ molecular ions in the ground ($X^2\Pi$) and in excited $a^4\Pi$, $A^2\Pi$ and $b^2\Sigma$ electronic states with appreciable vibrational excitation. In particular,

reactions with less energetic He*(2 ^{3}S) atoms show the propensity to give molecular ions mostly in the first excited electronic $a^4\Pi$ state; the vibrational excitation accompanies the formation of O_2^+ in the ground $X^2\Pi$ state [25]. However, much less information is available on the Ne* ($^3P_{2,0}$) + O_2 reaction stereodynamics.

For the Ne*($^3P_{2,0}$) –N_2 system some peculiarities of the vibrational and rotational state distributions of N_2^+ ionic product were provided by laser-induced fluorescence experiments [26]. Important features of the isotropic optical potential for Ne($^3P_{2,0}$) – N_2 were obtained from a multi-property analysis of several experimental data sets [27]. The study emphasized the necessity of using the combination of two imaginary components to reproduce simultaneously all the analyzed experimental observables that probe complementary details of the interaction. This necessity was related to the probable occurrence of two competitive ionization mechanisms. However, no details on the nature of the intermolecular forces involved and on the possible interconnection between real and imaginary parts of the optical potential was provided.

Basic aspects of the influence of atomic alignment on atom-molecule reaction stereodynamics, emerging both in the thermal and sub-thermal collision energy range, have recently been provided by experiments with Ne*($^3P_2$) atoms state selected in their magnetic sublevels [28,29]. However, a proper characterization of the dependence of structure and stability of the reaction TS on the molecular orientation is still lacking. An important further step forward is represented by the dependence of reactivity on the mutual orientation of both reagents as reported in this letter.

By exploiting preliminary considerations on the role of the nature and orientation of the molecular partner, we demonstrate that the stereodynamics of the Ne*($^3P_{2,0}$) + O_2 and Ne*($^3P_{2,0}$) + N_2 reactions are completely different. In particular, these reactions occur with mechanisms controlled by TSs whose different structures arise from the selective role of the intermolecular forces involved. Moreover, other emerging aspects are: i) CHEMI of O_2 provides a more efficient ionization compared to CHEMI of N_2; ii) O_2^+ molecular ions show the propensity to be formed in the first excited electronic state. Both these features are expected to affect substantially the balance of phenomena occurring in atmospheric environments [22,23].

3. Differences in the experimental findings

In previous work, total ionization cross sections have been measured in a crossed beam apparatus in the Perugia laboratory, already described in detail in previous papers [30–32]. In short, the apparatus consists of two beams of effusive character, one of metastable rare gas atoms, generated by electron bombardment, and the other one of the target molecules in the ground state, that cross at 90°. Product ions are extracted from the scattering volume by an external electric field (usually ≈ 150 V/cm).

For the total ion intensity measurements, ions are directly detected by a channel electron multiplier. For mass analysis, product ions are focused, mass filtered by a quadrupole, and detected by another channel electron multiplier.

A time-of-flight device was used to obtain the velocity (or collision energy) dependence of cross sections, including those of interest for the present study. A normalization/calibration procedure has been adopted to provide total ionization cross sections for several CHEMI systems involving both prototype inorganic and organic molecules, given in an internally consistent absolute scale [30–32]. The collision energy dependence of cross sections so determined for the selected systems, Ne ($^3P_{2,0}$) + O_2, N_2, and CO, are shown in Fig. 1 where cubic polynomial fits to the data are plotted, providing an interpolation of the experimental data [30]. The use of polynomial interpolation allows a direct comparison of the experimental findings characterized for many systems, since providing a better job of "guiding the eye" through several data sets. The figure shows that the energy dependence of the total ionization cross section for the two molecules of interest O_2 and N_2 is completely
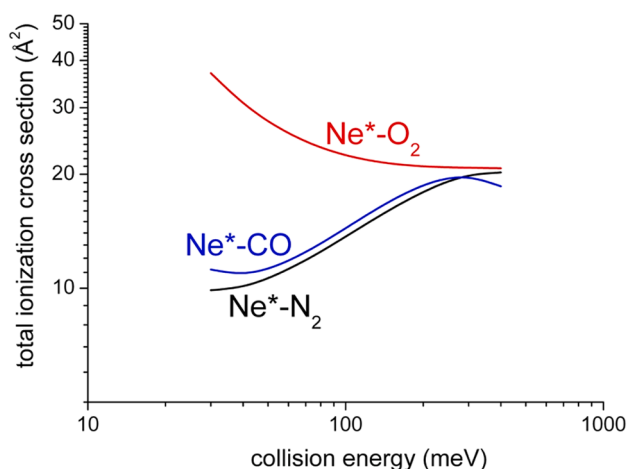

Fig. 1. Experimental total ionization cross sections of CHEMI reactions induced on N_2, CO and O_2 molecules by collisions with metastable Ne*($^3P_{2,0}$), plotted as a function of the collision energy. Each curve is a best fit to the real experimental data (see ref. [30]) represented by a third-degree polynomial, whose coefficients are obtained by a standard regression procedure.

different, while a strong similarity is shown for the CHEMI of N_2 and CO. Furthermore, the absolute value of the cross section for CHEMI of O_2, in the thermal range (30–40 meV), is at least a factor of 3 larger than those of both N_2 and CO molecules. The O_2 behavior is rather similar to that of Cl_2, for which we have recently discussed [33] the role of "harpooning" in the entrance channels of CHEMI.

4. Selectivity of the reaction channels

Important reaction selectivities that represent the main focus of the present investigation are suggested by the different chemical and physical properties of O_2 and N_2 reagent molecules that control the range, strength and anisotropy of the intermolecular forces involved. In particular, while their electronic polarizabilities α exhibit comparable values (α = 10.7 and 11.7 a.u. for O_2 and N_2, respectively) [34], their electric quadrupole moments Q_e are rather different (Q_e=- 0.3 and −1.1 a.u.) [35]. These features suggest that at large separation distance, while the dispersion attraction controlled by the polarizability must be similar for O_2 and N_2, the polarization component induced on the "floppy" outer electronic cloud of Ne* by the molecular Q_e is expected to be rather different. Moreover, the different chemical behavior of the interaction at short separation distance is expected to be modulated by the fact that O_2 in its ground electronic state $^3\Sigma_g^+$ is an open shell species with an ionization potential (I_p) of 12.071 eV, and a positive electron affinity (EA = 0.44 eV) [35], while N_2 in its ground state $^1\Sigma_g^+$ is a closed shell species with I_p = 15.581 eV and a negative EA. The modulation can be assessed taking into account also the different sequences of HOMO and LUMO orbitals shown in Fig. 2.

The energetic and open shell nature of Ne*($^3P_{2,0}$) and the features of N_2 and O_2 molecules generate important differences in the intermolecular forces involved, and according to the phenomenology of atom–atom reactions [16–18], this originates changes both in the real and imaginary parts of the optical potentials for the two systems. As a consequence, the manifold of reaction entrance and exit channels must be different and pronounced selectivity in the reaction dynamics are expected to occur. Some basic differences are depicted in Fig. 3, where the qualitative scheme of potential energy curves is obtained exploiting the asymptotic values of energy and correlation formulas developed in our
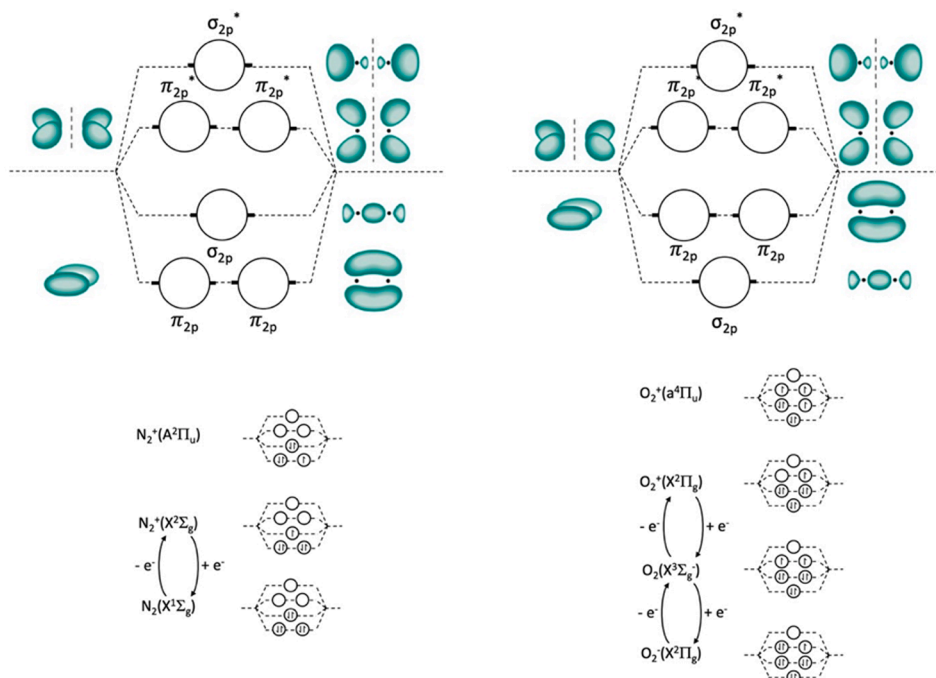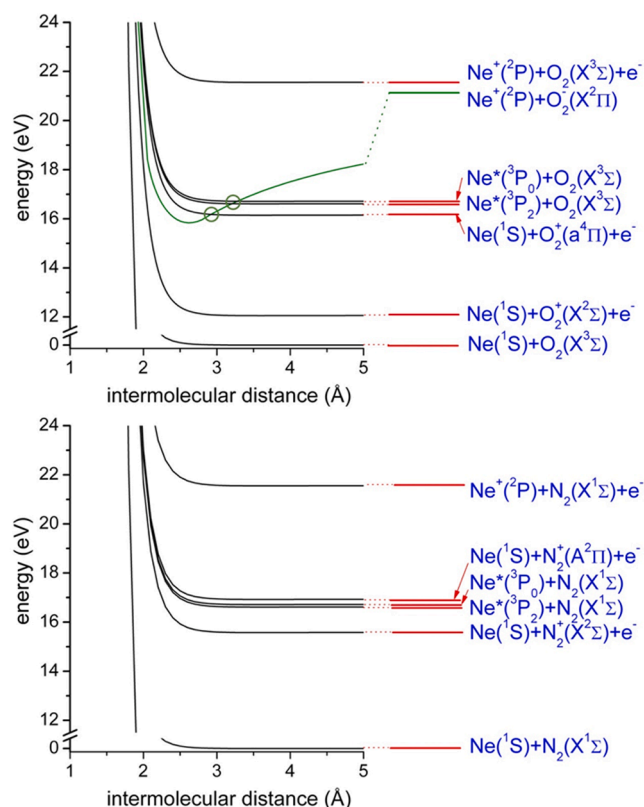

Fig. 3. The manifold of entrance and exit channels with a schematic view of the involved interaction potentials for Ne*–N_2 (lower panel) and Ne*–O_2 (upper panel) CHEMI reactions. In the potential energy curves reported in the upper panel the circles highlight the crossing regions between neutral and ionic states promoting the Ne$^+$–O_2^- ion pair formation (see text).

laboratory and reported in detail elsewhere [39]. Therefore, the comparison of molecular properties presented above and the interaction potential scheme given Fig. 3 suggest that while the long-range forces

Fig. 2. HOMO and LUMO molecular orbitals of N_2 (left panel) and O_2 (right panel) in neutral and ionic states involved in the interaction with Ne*($^3P_{2,0}$).

should be rather similar for these two systems, important differences are expected for the collision dynamics at short distances. In the processes that are mainly confined at intermediate and short distance range, ionization stereodynamics and TS, more directly controlled by the increased strength and anisotropy of the intermolecular forces and by symmetry and energetic of diatomic valence orbitals involved in the electron exchange, must substantially change in the two cases. In particular, real and imaginary parts of the optical potential, controlling respectively energy dependence and value of the total ionization cross section must be rather different.

The case of N_2 suggests that:

-Under low energy (sub-thermal and thermal) collision conditions, the anisotropic attraction due to the dispersion and induction interaction components tends to promote molecular alignment, more efficient for molecules in low lying rotational states, which leads to the collinear approach as the most stable configuration. Moreover, the 3 s electron orbital polarization in Ne* induced by the high permanent Q_e of N_2 on the "floppy" cloud, reveals the open shell nature of Ne^+ ionic core. Therefore, collisions occurring with impact parameters b sufficiently high, probing large intermolecular distances, are accompanied by an emerging polarization of the 3 s Ne* orbital, inducing *sp* and *spd* hybridization of outer Ne* orbitals [3], that triggers the *indirect* reaction mechanism. Spin-orbit and Coriolis effects also contribute to the imaginary part of the optical potential. In particular, the electric field associated with weak intermolecular forces breaks the validity of the optical selection rules, allowing ionization to occur by a concerted emission–absorption of a "virtual" photon within the complex formed by collision [17–20]. In contrast, collisions at low b probe the short-range potential where chemical forces driving the *direct* mechanism emerge. Some relevant features of the reaction transition state (TS) are depicted in Fig. 4. The charge transfer perturbation couples both $Ne^+–N_2$ and Ne-N_2^+ states, with their proper symmetry. The coupling by charge transfer is maximum for the collinear configuration, as previous work on the near resonant $Ar^+–N_2$ and Ar-N_2^+ states has shown [37]. Moreover, the collinear configuration of the TS leads to N_2^+ ion products in the ground electronic state (see Figs. 2 and 4) with possible vibrational and rotational excitation. Several studies on anisotropic systems have demonstrated that the collinear configuration favors the internal energy exchange between colliding partners (see for instance the recent ref. [38]).
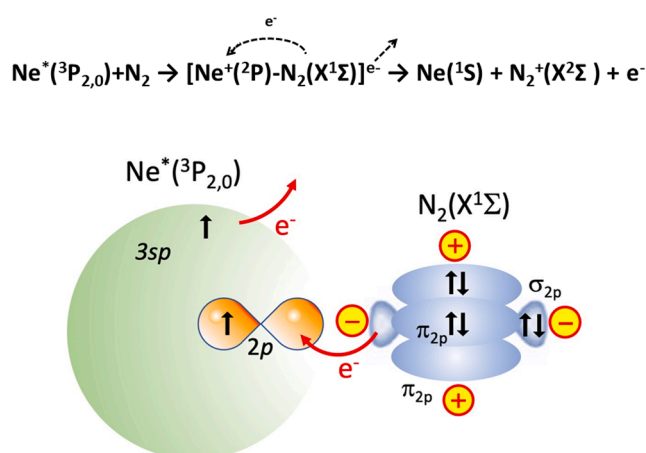
-In the case of fast collisions at higher energy and with rotationally excited neutral reagents, the molecular alignment induced by the anisotropy of the intermolecular forces is less efficient, allowing perpendicular configurations contribute to the reaction, promoting the opening of an additional channel. Under these conditions, the formation of N_2^+ electronically excited in the $A^2\Pi$ state can also occur, that requires the removal of one electron from the more internally occupied π_{2p} orbitals of N_2 which expose no nodal planes for a perpendicular approach of reagents (see Fig. 2).

Here, a different 3 s electron polarization emerges, similar to that operating in CHEMI involving heavier Ng [16–18], which leads to the formation of a TS where an ionic adduct in the perpendicular configuration is surrounded by a Rydberg electron.

In contrast, the O_2 system exhibits the following behavior:

- Under low energy (sub thermal and thermal) collision conditions, the 3 s electron polarization induced by the weaker permanent Q_e of O_2 is less efficient compared to the N_2 case. However, the partial *sp-spd* hybridization of the outer Ne* orbital and the appreciable molecular electron affinity can promote the formation of the Ne^+- O_2^- ion pair at the crossings between neutral and ionic states [25], as indicated in the upper panel of Fig. 3. *Non adiabatic* events at such crossings involve the transition from *singlet*, *triplet* and *quintet* states of the neutral entrance channels to *singlet* and *triplet* states of the intermediate $Ne^+–O_2^-$ ion pair and the final passage to the *triplet* state of the exit ionic channels, leading to the formation of $O_2^+(a^4\Pi) + e^-$ (s = 1/2) products. In this case two electrons are ultimately ejected by the O_2 molecular target, consistent with the participation of the transient anion O_2^-. In addition, the basic features of the overlap, that controls the removing of one electron from the internal π_{2p} molecular orbital and the simultaneous ejection of one electron from the more external occupied $\pi_{2p}*$, suggests that the reaction must preferentially occur in the perpendicular configuration (see Fig. 5).

These considerations indicate that the selectivity of charge transfer makes the *direct* mechanism dominant under several collision conditions, leading to distances of closest approach comparable or lower than 3 Å (see Fig. 3). Moreover, the structure of the TS, depicted in Fig. 5,
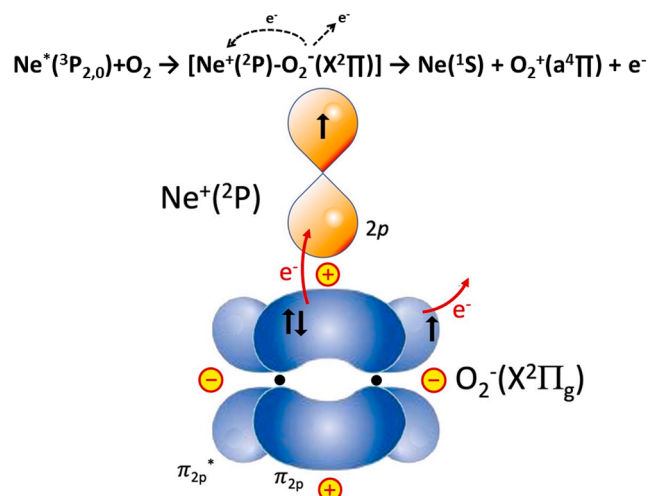

Fig. 4. Possible structure of the transition state of the Ne*–N_2 for the *direct* mechanism emerging at low collision energy (thermal and sub-thermal regimes) and low impact parameters b. The ionization occurs when the metastable Ne* atom approaches the N_2 molecule collinearly. In such a configuration the highest occupied σ_{2p} molecular orbital of N_2 can transfer one electron to the inner shell 2p vacancy of Ne*, leading to the ejection of the Rydberg electron. In this configuration, the negative pole of the N_2 quadrupole polarizes the Rydberg 3 s orbital, leading to 3*sp* and 3*spd* hybridization [3,20].

Fig. 5. Possible structure of the transition state of the Ne*–O_2 CHEMI reactions for the *direct* mechanism emerging at low collision energy (thermal and sub-thermal regimes). Here when the Ne* atom approaches the O_2 molecule, because of a curve crossing (see upper panel of Fig. 3), an electron is transferred from Ne* to O_2, and the ion pair $Ne^+–O_2^-$ is formed. Therefore, in this case the ionization occurs with two electrons leaving the O_2^- negative ion and the most favorable geometry is the one with Ne* perpendicularly approaching the diatom.

appears to be completely different compared to the case of N_2 (see Fig. 4); its perpendicular configuration emphasizes the selective role of the *direct* mechanism and justifies the small vibrational excitation of the O_2^+ product as previously observed [25].

- At high (hyper-thermal) collision energies, *diabatic* passages at crossings between neutral and ionic states become more efficient and some selectivity operating at low collision energies is lost. As with N_2, CHEMI of O_2 also tends to be promoted by all relative configurations of reagents and the balance of *direct* and *indirect* mechanisms becomes similar and comparable with that promoting atom–atom reactions [16–18].

5. Conclusions

In this letter it is found that important selectivity accompanies the stereodynamics of Ne*($^3P_{2,0}$) + O_2 and of Ne*($^3P_{2,0}$) + N_2 CHEMI reactions. Pronounced differences in the reaction probability emerge under thermal collision conditions where the Ne*–O_2 CHEMI reaction exhibits a total ionization cross section which is larger than a factor 3 with respect to that of Ne*–N_2. This basic experimental finding has not properly rationalized in previous studies. Moreover, the reaction with N_2 involves a critical balance of *direct* and *indirect* mechanisms and leads to N_2^+ in the ground electronic state $^2\Sigma_g^+$ with the propensity to be vibrationally and rotationally excited since the relevant TS preferentially assumes a collinear configuration which couples with inelastic events [38]. On the other hand, the CHEMI involving O_2 is driven by a more efficient *direct* mechanism that is controlled by stronger chemical forces. In particular, in the entrance channels the O_2 reagent first undergoes a reduction to O_2^- and subsequently an oxidation to O_2^+ in its first excited electronic state a$^4\Pi_u$ with limited vibrational excitation and the relevant TS in a perpendicular configuration.

A recent experimental paper [39] emphasizes that further basic differences characterize the stereodynamics of Ne*($^3P_2$) + N_2 and Ne* ($^3P_2$) + CO CHEMI reactions, leading to different associative to Penning branching ratio at sub-thermal collision energy. Interestingly, within the general view proposed in this work, the ionization potential value of CO (I_p = 14.014 eV) is intermediate between those of N_2 and O_2. CO molecule shows also permanent electric dipole (0.11D) and quadrupole (-1.5 a.u.) moments, a polarizability (α = 13.1 a.u.) slightly higher respect to those of N_2 and O_2, a HOMO orbital mainly confined on the C atom and the first excited state of CO$^+$ easily accessible, occurring at 16.583 eV. Therefore, the proper identification of the intermolecular forces driving the CO CHEMI can cast light on the effect of the molecular asymmetry on the reaction stereodynamics.

As a final comment, it can be stressed that starting from the suggestions of the present paper our next target is the formulation of new and complete optical potential for Ne*(^3P_J) + N_2 system, that includes in an internally consistent way both real and imaginary part in order to properly represent all entrance and exit reaction channels. Particular attention is focused on the combined role of atomic alignment and of molecular orientation on the reaction streodynamics emerging at different collision energies. This is a necessary condition to carry out state-to-state reaction dynamical studies providing a unifying rationalization of the available experimental observables. The detailed investigation of this prototype case is priority for the extension of the study to the other molecular systems.

Declaration of Competing Interest

The authors declare that they have no known competing financial interests or personal relationships that could have appeared to influence the work reported in this paper.

References

[1] F. Nunzi, G. Pannacci, F. Tarantelli, L. Belpassi, D. Cappelletti, S. Falcinelli, F. Pirani, Molecules 25 (2020) 2367.
[2] P.E. Siska, Adv. Chem. Phys. 45 (1981) 488.
[3] P.E. Siska, Rev. Mod. Phys. 65 (1993) 337.
[4] B. Brunetti, F. Vecchiocattivi, Autoionization Dynamics of Collisional Complexes. In Current Topic on Ion Chemistry and Physics (Eds: C. Y. Ng, T. Baer, I. Powis), John Wiley & Sons Ltd, New York (1993) 359.
[5] O. Dulieu, A. Osterwalder, Cold Chemistry, Molecular Scattering and Reactivity Near Absolute Zero, Royal Society of Chemistry, Cambridge, 2018, pp. 1–670.
[6] H.A. Bethe, Phys. Rev. 57 (1940) 1125.
[7] H. Hotop, A. Niehaus, Chem. Phys. Lett. 8 (1971) 497–500.
[8] K. Ohno, H. Mutoh, Y. Harada, J. Am. Chem. Soc. 105 (1983) 4555–4561.
[9] P.E. Siska, J. Chem. Phys. 85 (1986) 7497–7498.
[10] S. Schohl, M.W. Müller, H.A.J. Meijer, M.-W. Ruf, H. Hotop, H. Morgner, Z. Phys. D 16 (1990) 113–130.
[11] M. Yamato, S. Okada, V. Wei-Keh Wu, H. Ohoyama, T. Kasai, J. Chem. Phys. 113 (2000) 6673–6676.
[12] A. B. Henson, S. Gersten, Y. Shagam, J. Narevicius, and E. Narevicius, Science338 (2012) 234-238.
[13] E. Lavert-Ofir, Y. Shagam, A.B. Henson, S. Gersten, J. Kłos, P.S. Zuchowski, J. Narevicius, E. Narevicius, Nat. Chem. 6 (2014) 332–335.
[14] S.D.S. Gordon, J. Zou, S. Tanteri, J. Jankunas, A. Osterwalder, Phys. Rev. Lett. 119 (2017), 053001.
[15] B. Brunetti, P. Candori, S. Falcinelli, B. Lescop, G. Liuti, F. Pirani, F. Vecchiocattivi, Eur. Phys. J. D 38 (1) (2006) 21–27.
[16] S. Falcinelli, F. Vecchiocattivi, F. Pirani, Phys. Rev. Lett. 121 (2018), 163403.
[17] S. Falcinelli, F. Vecchiocattivi, F. Pirani, Comm. Chem. 3 (2020) 64.
[18] S. Falcinelli, J.M. Farrar, F. Vecchiocattivi, F. Pirani, Acc. Chem. Res. 53 (2020) 2248.
[19] M.H. Miller, H. Morgner, J. Chem. Phys. 67 (1977) 4923.
[20] R.W. Gregor, P.E. Siska, J. Chem. Phys. 74 (1981) 1078.
[21] S. Falcinelli, A. Bartocci, S. Cavalli, F. Pirani, F. Vecchiocattivi, Chem. Eur. J. 22 (2016) 764.
[22] S. Falcinelli, F. Pirani, F. Vecchiocattivi, Atmosphere 6 (2015) 299–317.
[23] M. Alagia, N. Balucani, P. Candori, et al., Rend. Lincei Sci. Fis. Nat. 24 (2013) 53–65.
[24] F.T.M. van den Berg, J.H.M. Schonenberg, H.C.W. Beijerinck, Chem. Phys. 115 (1987) 359.
[25] O. Leisin, H. Morgner, W. Müller, Z. Phys, A 304 (1982) 23.
[26] D.M. Sonnenfroh, S. Leone, Int. J. Mass. Spectr. Ion Proc. 80 (1987) 63.
[27] J. Baudon, P. Feron, C. Miniatura, F. Perales, J. Reinhardt, J. Robert, H. Haberland, B. Brunetti, F. Vecchiocattivi, J. Chem. Phys. 95 (1991) 1801.
[28] J. Zou, S.D.S. Gordon, S. Tanteri, A. Osterwalder, J. Phys. Chem. 148 (2018), 164310.
[29] J. Zou, S.D.S. Gordon, A. Osterwalder, Phys. Rev. Lett. 123 (2019), 133401.
[30] A. Aguilar, B. Brunetti, M. Gonzalez, F. Vecchiocattivi, Chem. Phys. 145 (1990) 211.
[31] B. Brunetti, S. Falcinelli, S. Paul, F. Vecchiocattivi, G.G. Volpi, J. Chem. Soc., Faraday Trans. 89 (1993) 1505.
[32] N. Balucani, A. Bartocci, B. Brunetti, P. Candori, S. Falcinelli, F. Palazzetti, F. Pirani, F. Vecchiocattivi, Chem. Phys. Lett. 546 (2012) 34–39.
[33] S. Falcinelli, F. Vecchiocattivi, J.M. Farrar, F. Pirani, J. Phys. Chem. A 125 (16) (2021) 3307–3315.
[34] T.N. Olney, N.M. Cann, G. Cooper, C.E. Brion, Chem. Phys. 223 (1997) 59.
[35] A.A. Radzig, B.M. Smirnov, Reference Data on Atoms, Molecules and Ions, Springer, Berlin, 1985.
[39] J. Zou, A. Osterwalder, J. Phys. Chem. 153 (2020), 104306.
[37] R. Candori, S. Cavalli, F. Pirani, A. Volpi, D. Cappelletti, P. Tosi, D. Bassi, J. Chem. Phys. 115 (2001) 8888–8898.
[38] Q. Hong, Q. Sun, M. Bartolomei, F. Pirani, C. Coletti, PCCP 22 (2020) 9375–9387.
[36] F. Pirani, G.S. Maciel, D. Cappelletti, V. Aquilanti, Int. Rev. Phys. Chem. 25 (2006) 165–199.